Title

Hyperbranched Unsaturated Polyphosphates as a Protective Matrix for Long-Term Photon Upconversion in Air

Journal

Journal of the American Chemical Society, 136(31)

ISSN

0002-7863

Authors

Marsico, Filippo
Turshatov, Andrey
Peköz, Rengin
et al.

Publication Date

2014-08-06

DOI

10.1021/ja5049412

Peer reviewed

JACS
JOURNAL OF THE AMERICAN CHEMICAL SOCIETY

Article

pubs.acs.org/JACS

Hyperbranched Unsaturated Polyphosphates as a Protective Matrix for Long-Term Photon Upconversion in Air

Filippo Marsico,[†,§] Andrey Turshatov,[†] Rengin Peköz,[†] Yuri Avlasevich,[†] Manfred Wagner,[†] Katja Weber,[†] Davide Donadio,[†] Katharina Landfester,[†] Stanislav Baluschev,[†,‡] and Frederik R. Wurm*[,†]

[†]Max Planck Institute for Polymer Research, Ackermannweg 10, 55128 Mainz, Germany

[‡]Optics and Spectroscopy Department, Faculty of Physics, Sofia University "St. Kliment Ochridski", 5 James Bourchier, 1164 Sofia, Bulgaria

[§]Graduate School of Excellence "Materials Science in Mainz", Staudinger Weg 9, 55128 Mainz, Germany

Supporting Information

ABSTRACT: The energy stored in the triplet states of organic molecules, capable of energy transfer via an emissive process (phosphorescence) or a nonemissive process (triplet–triplet transfer), is actively dissipated in the presence of molecular oxygen. The reason is that photoexcited singlet oxygen is highly reactive, so the photoactive molecules in the system are quickly oxidized. Oxidation leads to further loss of efficiency and various undesirable side effects. In this work we have developed a structurally diverse library of hyperbranched unsaturated poly(phosphoester)s that allow efficient scavenging of singlet oxygen, but do not react with molecular oxygen in the ground state, i.e., triplet state. The triplet–triplet annihilation photon upconversion was chosen as a highly oxygen-sensitive process as proof for a long-term protection against singlet oxygen quenching, with comparable efficiencies of the photon upconversion under ambient conditions as in an oxygen-free environment in several unsaturated polyphosphates. The experimental results are further correlated to NMR spectroscopy and theoretical calculations evidencing the importance of the phosphate center. These results open a technological window toward efficient solar cells but also for sustainable solar upconversion devices, harvesting a broad-band sunlight excitation spectrum.

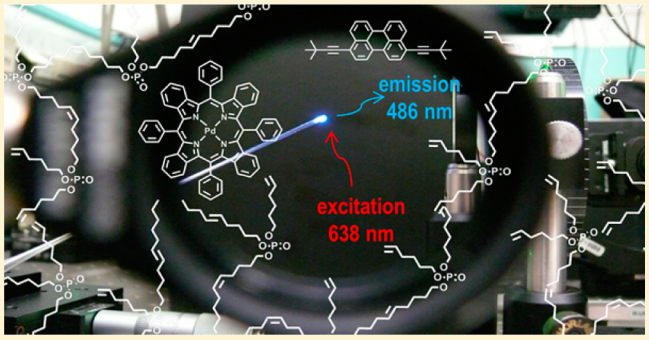

INTRODUCTION

Singlet oxygen is a highly reactive form of molecular oxygen that is generated in many photonic processes, typically photosensitized when triplet energy is transferred to environmental, i.e., triplet, oxygen, promoting its energy to the singlet state.[1] Highly reactive singlet oxygen rapidly reacts with organic molecules. Although it can be profitably used in photodynamic cancer therapies,[1−4] in many processes its destructive oxidation is highly unwanted. Thus, many strategies exist to exclude oxygen from photoprocesses by passive protection, i.e., by encapsulation of the active compounds in polymer films[5] or nano- and microcarriers[6−10] to reduce oxygen permeability. These strategies are effective for minutes or hours, but are insufficient for technological application due to their still very short lifetimes. Also, the use of glass-packaged samples, prepared and sealed in an inert atmosphere glovebox, restricts the application potential considerably due to high costs and inflexible packaging. Also, the straightforward active protection strategy, namely, the addition of oxygen scavengers in molar concentrations, is ineffective. In fact, relatively short device lifetimes, on the order of hours or single days, were achieved, as conventional antioxidants also react with normal atmospheric triplet oxygen and are consumed too fast.[11]

We have developed a series of synthetic hyperbranched unsaturated poly(phosphoester)s (hbUPPEs) that actively scavenge singlet oxygen but do not react with oxygen in the triplet ground state (Scheme 1), which makes these compounds ideal synthetic matrixes for photoactive molecules. Different branched polymers with varying branching densities are synthesized in a one-step polymerization from the respective A_3-type monomers, which are accessible in one step from phosphorus oxychloride and are polymerized via olefin metathesis polymerization (see below). To investigate the oxygen-scavenging properties of these novel materials, we chose the triplet–triplet annihilation photon upconversion (TTA-UC) as a highly oxygen-sensitive photonic process. TTA-UC is the only upconversion method that has been experimentally demonstrated to operate with noncoherent low-intensity illumination such as sunlight. Our results are therefore highly important for all applications that have to be conducted in (or

Received: May 17, 2014
Published: July 10, 2014

   dx.doi.org/10.1021/ja5049412 | J. Am. Chem. Soc. 2014, 136, 11057−11064

with) sunlight (e.g., coatings or solar energy devices).[12] TTA-UC is a unique process that allows the generation of high-energy photons from lower energy excitation photons at very low intensity and extremely low spectral power density of the optical source used.[5,8,13] It has been demonstrated that moderate concentrated sunlight can fulfill the energy requirements for effective TTA-UC, thus allowing the development of several unique applications in material science, solar cell devices, solar fuels, and bioimaging under mild excitation conditions, which are, however, all highly oxygen-sensitive.[8,10−12,14]

The TTA-UC process (Figure 1) is based on the energy transfer between the optically created triplet ensembles of the

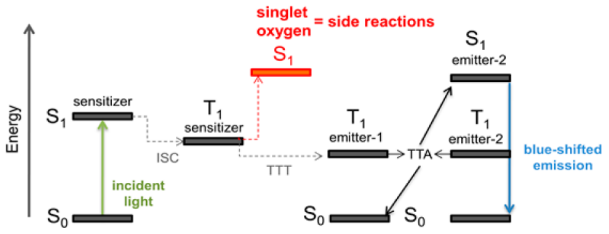

Figure 1. Schematic energy-level diagram of triplet−triplet annihilation photon energy upconversion (gray pathway). The process involves population of the first singlet excited state of a sensitizer (S_1) upon absorption of incident light, intersystem crossing (ISC) to the triplet excited state (T_1), triplet−triplet energy transfer (TTT) from the sensitizer to an emitter (T_1), and triplet−triplet annihilation (TTA) of two emitter triplets to populate the emitter excited singlet state (S_1), which decays by delayed fluorescence (blue shift). In the presence of molecular oxygen, the excited triplet states (T_1) are quenched effectively (red pathway).

sensitizer molecules (usually metalated macrocycles) to accessible triplet states of the emitter molecules (conjugated hydrocarbons). Processes that cause depopulation of either of these triplet energy reservoirs imply a loss mechanism and decrease the efficiency of the TTA-UC process: under ambient conditions no UC is observed. The most important loss mechanism usually involves oxygen and prevents the application of UC in air at ambient conditions (Figure 1, red pathway). Both sensitizer and emitter ensembles can also transfer their triplet excitation to molecular oxygen, and consequently, the efficiency of the upconversion process is much lower.[2,15] Furthermore, the hereby generated singlet oxygen is highly reactive, leading to oxidation of the sensitizer and emitter molecules.

We have recently developed a versatile platform to produce various linear poly(phosphoester)s via olefin metathesis.[16−18] Here, we present the development of a structurally diverse library of the first hbUPPEs working as an active and passive protective matrix to perform highly efficient upconversion under ambient conditions (Figure 2). A clear structure−property relationship between the polymer architecture and the UC efficiency was demonstrated by a combination of measurements and theoretical calculations. TTA-UC was demonstrated to occur in ambient conditions in a polymeric matrix with efficiencies comparable to the corresponding standard value for systems assembled under glovebox conditions. The possibility to tune chemical and physical properties in rubbery materials can have a strong impact on a variety of technologies, including photovoltaics on a market scale, due to their long lifetime and due to the versatile postpolymerization functionalization of hyperbranched polymers.

RESULTS AND DISCUSSION

Structural Design and Synthetic Strategy. Hyperbranched (hb), i.e., statistically branched, polymers are considered as materials suitable for large-scale applications in coatings or resins, as they are synthesized in a single polymerization step yielding highly functional materials with peculiar properties for coatings, drug carriers, etc.[19,20] Herein, we extend their applications toward highly efficient active−passive protectors to allow TTA-UC in an ambient atmosphere that can be applied in future solar cells or for bioimaging. A branch-on-branch structure with a large number of terminal groups gives excellent flow and processing properties to these polymers superior to most linear polymers.[19] From the early beginning, different methodologies have been developed for the synthesis of hb polymers: step-growth polymerization techniques are probably the most frequently applied strategies.[21,22] Generally, these approaches are based on AB_n monomers in which the single A group reacts ideally only with the B groups of the monomer via polycondensation or polyaddition. The polymerization of a mixture of monomers of type A_2/B_3 also leads to highly branched structures often based on commercially available materials.[22] The branched structure leads to amorphous materials, since branching prevents crystallization, resulting in low viscosities both in the bulk and in solution.[22] In spite of the above-mentioned benefits, harsh reaction conditions often need to be applied for the synthesis of hb polymers by polycondensation. Recently, olefin metathesis was used to prepare hb polymers under mild conditions.[23,24] Olefin metathesis is able to polymerize an A_3 monomer without the need for a complementary B_2 monomer. This was first shown by the group of Meier with polymerization of a glyceryl triundec-10-enoate to yield highly branched materials.[25,26] Control over the molecular weight during the hyperbranching polymerization of suitable A_3 monomers is achieved by the addition of chain stoppers to perform the one-step and one-pot reaction and to prevent cross-linking.

The structural versatility of phosphorus gives fast access to A_3 monomers, with the phosphate being the branching point that can undergo acyclic triene metathesis (ATMET) to produce hbUPPEs. The herein reported monomers are the first phosphates for ATMET polymerization reported to date: tribut-3-en-1-yl phosphate (**1**), trihex-5-en-1-yl phosphate (**2**), and triundec-10-en-1-yl phosphate (**3**) were investigated as monomers with variable chain length between the double bond and the phosphate branching unit to vary the branching point density within the hb polymers (Scheme 1). These A_3 monomers were polymerized with the Grubbs first-generation catalyst in the bulk, avoiding gelation by fine-tuning the reaction temperature and catalyst amount and to produce soluble branched materials.

The high number of terminal double bonds, combined with the low glass transition temperatures (ca. −80 to −90 °C) of the hbUPPEs, provides a mobile and closed matrix for the dispersion of the hydrophobic dyes (palladium porphyrins and perylene derivatives; see below) that are necessary for TTA-UC.

The metathesis of **1** was used as a model monomer to study the growth of the olefin-rich hbUPPEs without a complementary B_2-type monomer in the presence of the appropriate ruthenium catalyst. The polymerization of **1** can be followed by

dx.doi.org/10.1021/ja5049412 | J. Am. Chem. Soc. 2014, 136, 11057−11064

Scheme 1. Schematic Representation of Monomer Synthesis and ATMET Polymerization Conditions for the Synthesis of hbUPPEs

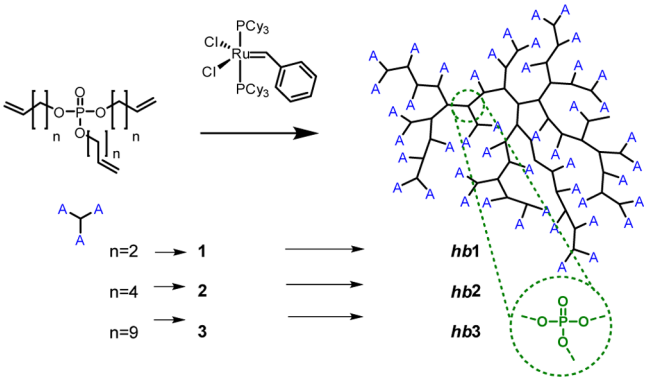

^{1}H NMR as the terminal olefin resonances of the monomer at 5.8 and 5.1 ppm change into much broader peaks after polymerization and also internal polymeric double bonds (at ca. 5.5 ppm) can be detected (Figure 2). These results prove, combined with SEC (size exclusion chromatography) equipped with a viscosity detector, the highly branched and polyfunctional structure of the hbUPPEs.

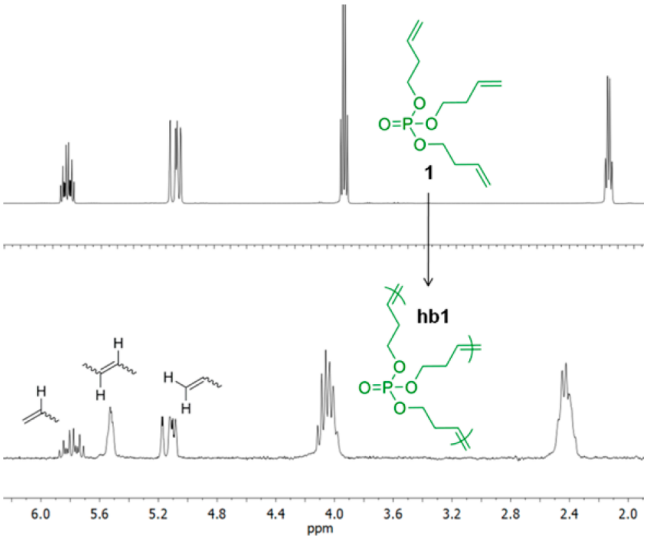

Figure 2. ^{1}H NMR (500 MHz in $CDCl_3$ at 298.3 K) showing a high level of terminal end group functionality after the controlled metathesis polymerization of **1**.

Since the monomers are liquid at room temperature, the polymerizations were carried out in the bulk by the addition of the appropriate amount of catalyst (usually 0.1−0.5 mol %) under argon. Considering molecular weight dispersity, for a linear ADMET system a value of M_w/M_n = 2 is the most probable distribution for a linear polycondensation, as conversion reaches 100%.[27] Nonlinear polycondensations, such as the metathesis of acyclic trienes, lead to systems with higher dispersity values.[19] In our case, highly branched UPPEs can be prepared with controllable molecular weights to achieve molecular weight dispersities that do not limit the UC applications, as discussed later.

From ^{31}P NMR spectroscopy a branched structure of the polymers can also be assumed, as several resonances are detected for **hb1** as a broad signal for the phosphates, depending on their position (linear, dendritic, terminal) within the branched polymer (see the Supporting Information).

Kinetics of Polymerization and Structural Considerations. To control the polymerization of A_3-type monomers and to prevent cross-linking of the materials, temperature has a key role as a control parameter. As shown in Scheme 1, this strategy without using a chain stopper ensured a high number of terminal double bonds while keeping the material soluble and preventing cross-linking. The polymerization of **1** was conducted in the presence of 0.5 mol % Grubbs first-generation (G1) catalyst at 40−45 °C under vacuum in the absence of solvent and monitored by SEC (Figure 3). Polymers **hb1** were

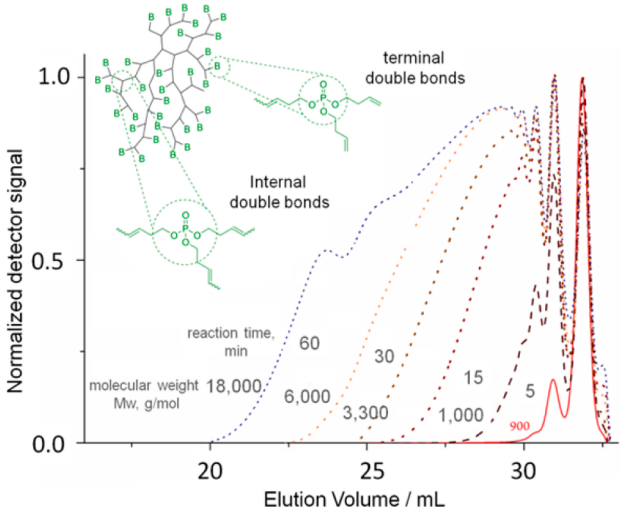

Figure 3. Size exclusion chromatography elugrams showing the kinetics of the polycondensation of **1** over a period of 140 min (0.8 mol % G1 catalyst, 30 °C).

obtained after several minutes with increasing molecular weight and molecular weight dispersities up to 90 min of reaction time (with M_w values of ca. 16000−18000 g mol^{-1} from SEC) and without cross-linking.

Because of the low viscosity of **hb1**, stirring was still possible after consumption of the monomer, ensuring homogeneous mixing with a quantitative monomer conversion. The polymerization of trihex-5-en-1-yl phosphate (**2**) and triundec-10-en-1-yl phosphate (**3**) reached apparent molecular weights of 16000 g/mol in a comparable reaction time, resulting in glassy transparent materials (**hb2**, **hb3**) after purification (Table 1).

The materials prepared herein showed high solubility in common organic solvents such as chloroform, benzene, toluene, and tetrahydrofuran with a low viscosity in solution. SEC equipped with a viscosity detector further proves the

Table 1. Characterization Data of hbUPPEs

hbUPPE	M_w[a]	M_n[a]	$Đ$[b]	α[c]	T_g[d]
hb1	18000	7000	2.6	0.44	−85
hb2	15500	3500	4.4	0.26	−88
hb3	20500	5600	3.7	0.17	

[a]In grams per mole, determined by SEC in THF vs polystyrene standards. [b]$Đ = M_w/M_n$, molecular weight dispersity from SEC. [c]Kuhn−Mark−Houwink parameter (determined from SEC/viscosimetry experiments in THF). [d]Glass transition temperature T_g (from DSC).

dx.doi.org/10.1021/ja5049412 | J. Am. Chem. Soc. 2014, 136, 11057−11064

highly branched structures as all Kuhn–Mark–Houwink parameters of the hbUPPEs are lower than 0.5, as is common for branched polymers.[28]

Triplet–Triplet Annihilation Photon Upconversion in hbUPPEs. The hbUPPEs can be used as a matrix to dissolve sensitizers and emitters for TTA-UC; the process can then be performed with high efficiencies under an ambient atmosphere. A crucial point for technological applications and device production is the lifetime of the oxygen protection. The long-term stabilities in an ambient atmosphere of the UC couples palladium tetrabenzoporphyrin (PdTBP) with 3,10-bis(3,3-dimethylbut-1-yn-1-yl)perylene (Y805) (Figure 4) in the different hbUPPEs were investigated.

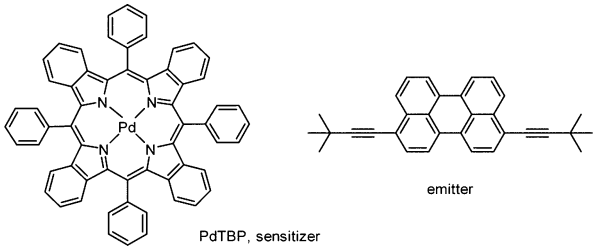

Figure 4. Chemical structures of palladium tetrabenzoporphyrin (sensitizer, left) and 3,9(10)-bis(3,3-dimethylbut-1-yn-1-yl)perylene (emitter, right) used herein for triplet–triplet annihilation photon upconversion.

The hbUPPEs were selected because of their optical transparency and suitable mechanical properties. The amorphous structure and low glass transition temperature impart a rubbery behavior as well as the possibility to obtain polymer matrixes with a high dye content. A crucial point for the matrix, besides the solubility of both dyes, is the fine-tuning of the length of the alkenyl chain to achieve high efficiency of the TTA-UC process. As demonstrated in Figure 5, all polymers (**hb1**, **hb2**, and **hb3**) can be used as a matrix for TTA-UC with high quantum yields (QYs) in an oxygen-rich environment.

As shown in Figure 6, the hbUPPEs demonstrate extremely efficient protection against quenching of the excited triplet

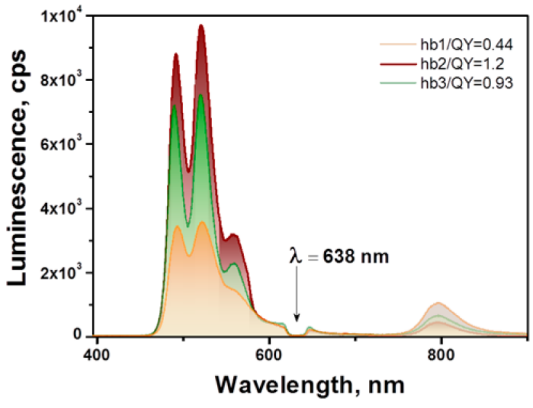

Figure 5. Luminescence spectra of polymer UC films in an ambient atmosphere (21% O_2): dark red, PdTBP/3,10-bis(3,3-dimethylbut-1-yn-1-yl)perylene/**hb2**; green, PdTBP/3,10-bis(3,3-dimethylbut-1-yn-1-yl)perylene/**hb3**; orange, PdTBP/3,10-bis(3,3-dimethylbut-1-yn-1-yl)perylene/**hb1** (excitation wavelength λ = 638 nm, light intensity ~100 mW cm^{-2}, thickness of all samples $d \approx 100$ μm, $c_{sensitizer} = 1 \times 10^{-4}$ mol L^{-1}, and $c_{emitter} = 2 \times 10^{-3}$ mol L^{-1}.

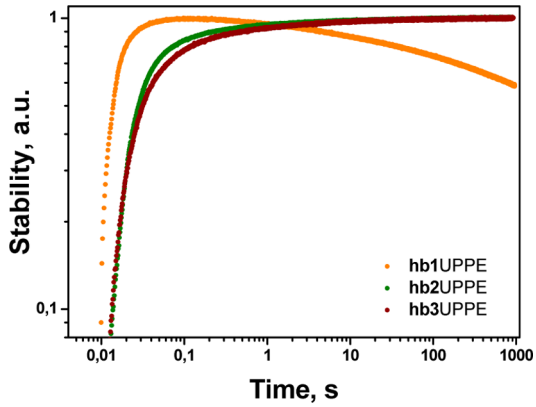

Figure 6. Long-term stability of the integral UC–fluorescence of the system PdTBP/3,10-bis(3,3-dimethylbut-1-yn-1-yl)perylene/**hb1,2,3** in an ambient atmosphere (21% O_2) for continuous irradiation with an excitation intensity of 100 mW cm^{-2}. UC was observed in a 100 μm polymer film under an ambient atmosphere.

states from molecular oxygen. Interestingly, **hb2** and **hb3** ensure almost undisturbed operation of TTA-UC in an ambient atmosphere for more than 1000 s (Figure 6, also Figure S24 (Supporting Information) for longer experiment times), while **hb1** does not provide effective long-term protection against oxygen quenching (Figure 6). In addition, a linear UPPE (compare Figures S25–S27, Supporting Information) was investigated for UC in an ambient atmosphere and found to be inferior to all branched UPPEs.

These high UC efficiencies in thin hbUPPE films under ambient conditions (Figure 6) allow simplification of the assembly of UC devices as no inert atmosphere is necessary. To establish the universal oxygen protective behavior of the new hbUPPE matrix, additional UC systems based on various emitters and sensitizers were investigated in the hyperbranched polymers (cf. Figures S21–S23 in the Supporting Information).[29,30] Indeed, each of the UC systems, which are typically well-soluble in organic solvents and only generate a UC signal in the absence of oxygen, work efficiently in the hbUPPEs under ambient conditions (as expected for viscous materials—such as the hbUPPEs—TTA-UC is less efficient than in an organic solvent (in the absence of oxygen); the respective quantum yields are reported in the Supporting Information, Table S1).

The efficient protection against oxygen quenching is most likely due to two effects: (i) an active chemical protection by scavenging singlet oxygen by the double bonds of the polymer which is present in the matrix from the beginning and (ii) an intrinsic passive protection of the viscous polyester matrix hindering oxygen diffusion, which has been reported for other hb polyesters before.[31]

Molecular Mechanism of Singlet Oxygen Scavenging. It is well-known that singlet oxygen reacts readily with olefins.[31] The particular reaction depends on the nature of the double bonds as different types of addition reactions (epoxides, dioxetanes, alcohols, etc.) can be generated as well as potential electron transfer reactions.[32,33] The purpose of an oxygen scavenger, i.e., active protection, is to minimize the amount of oxygen available for deteriorative reactions, leading to reduced functionality or degradation of the product. Further limitation of the oxygen amount is obtained by packaging, sealing, or encapsulation of the active substances, i.e., passive protection. For foods and pharmaceutical products, deteriorative reactions

dx.doi.org/10.1021/ja5049412 | J. Am. Chem. Soc. 2014, 136, 11057–11064

include lipid oxidation, nutritional loss, changes in flavor and aroma, alteration of texture, and microbial spoilage.[34] Typically, antioxidants are mixed within products to actively remove oxygen, while a protection strategy particularly designed for photochemical processes and especially for TTA-UC has not been described until now. The hbUPPEs inherently combine both strategies: namely, passive protection as a consequence of low oxygen permeability and active protection by chemical scavenging of the existing singlet oxygen while being rather inert against triplet oxygen.[31,34]

From the experimental results shown above, theoretical calculations as well as NMR studies were conducted to understand the efficiency of the hbUPPEs in oxygen scavenging. From NMR studies it can be concluded that the dipole interaction of the protons, carbons, and phosphorus atoms with the unpaired spins of oxygen leads to a change in the respective relaxation times depending on the distances of both. The measured relaxation times of the double bond protons show a strong dependency on the oxygen concentration (Figure 7). The increased relaxation times of the

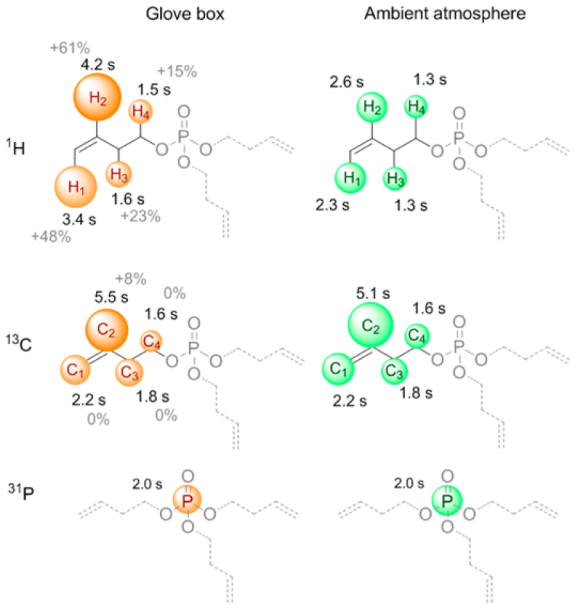

Figure 7. T_1 relaxation times of tribut-3-en-1-yl phosphate (**1**) at different oxygen levels quantified by ^{1}H, ^{13}C, and ^{31}P NMR (ambient atmosphere, 21% O_2; glovebox, 2 ppm of O_2).

butenyl fragment by approximately 48% (H_1), 61% (H_2), 23% (H_3), and 15% (H_4) under glovebox conditions (i.e., oxygen-free) compared to the relaxation times in air suggest a strong interaction with the partially paramagnetic oxygen for ambient atmosphere oxygen concentrations. The biggest effects are concentrated on the carbon−carbon double bond, which suggests an interaction of the free electrons of O_2 molecules with the π-orbitals of the double bond.

To understand the effect of the central atom on the reactivity and oxygen-scavenging ability of **hb2**, we investigated the effect of substituting the central phosphorus with boron, carbon, and nitrogen in the monomer precursors to the **hb2** unsaturated polymers by means of first-principles electronic structure calculations. The distribution patterns of the highest occupied molecular orbitals (HOMOs) and lowest unoccupied molecular orbitals (LUMOs) of **2** are displayed in Figure 8. In the case of B, C, and P, HOMOs are mostly localized on the terminal C−C

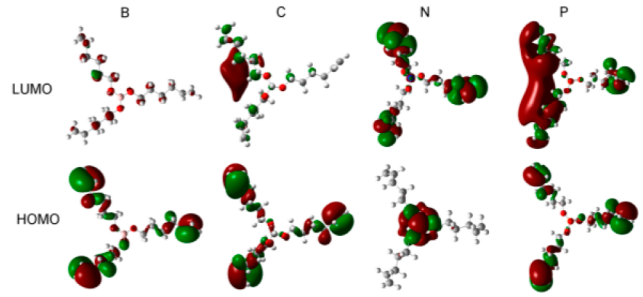

Figure 8. Distributions of the HOMO and LUMO for **2**. The central atom of the molecule is replaced with B, C, N, and P. The positive and negative values are shown in green and red, respectively, with an isosurface value of ±0.02 au.

double bonds, while the N-substituted case is an exception and HOMO is localized on the lone pair of the central N atom. On the other hand, LUMOs are completely different, depending on the central atom. The LUMO of the B-substituted molecule is completely delocalized with no specific preference, whereas C substitution yields a more localized LUMO distribution between two branches. For the N-substituted molecule the LUMO is mainly localized on the terminal double bonds and decreasing toward the center. However, the most significant LUMO distribution is found for the P-substituted molecule: the LUMO is delocalized between two terminal C−C double bonds of two different side chains of the molecule. These calculations show that, as the HOMO and the LUMO are localized in the same region of the molecule, hbUPPEs, i.e., **hb2**, are significantly more reactive toward singlet oxygen than other materials that are structurally very similar, but do not carry a P as the central atom.

The energetics of the oxygen-scavenging reaction and its atomistic mechanism were also studied by first-principles calculations (Figure 9). An **hb2** dimer in a cis configuration

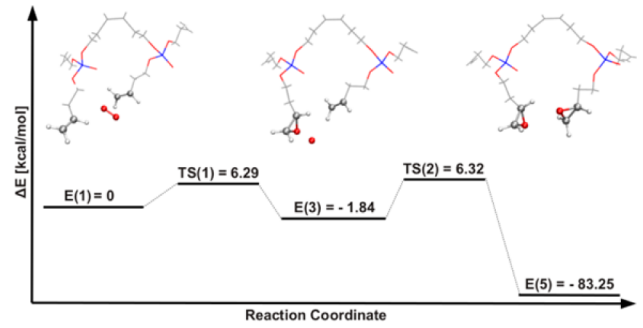

Figure 9. Computed reaction profile. Energies are in kcal/mol. Nonparticipating parts of the molecules in the reaction are omitted for clarity.

is considered, interacting with an O_2 molecule excited in the singlet state. Since the most reactive parts of these molecules are the terminal double bonds, we considered the reaction of O_2 with the C=C bonds. We found that the most stable product is an epoxide and that the reaction occurs in two steps. The first step involves the reaction of O_2 with one of the terminal C=C double bonds, leading to a metastable intermediate configuration (3 as shown in Figure 9). This step involves an activation barrier of 6.30 kcal mol^{-1}, and the intermediate has a relative energy of −1.84 kcal mol^{-1} with respect to the initial configuration. In the final product, the

dx.doi.org/10.1021/ja5049412 | J. Am. Chem. Soc. 2014, 136, 11057−11064

remaining oxygen atom is bonded to the second C=C bond available.

The second step is eased by the flexibility of the unsaturated side chains. The formation of the final configuration is not only energetically favored with an energy of −83.3 kcal/mol with respect to the starting and intermediate configurations but also kinetically accessible with an activation barrier of 6.3 kcal/mol.

CONCLUSION

In summary, we demonstrate the first synthesis of a family of hyperbranched unsaturated poly(phosphoester)s, with the phosphate groups being the branching points, and investigate their properties as scavengers for singlet oxygen. The polymer library was varied with respect to the branching point density via the alky spacer lengths in the monomers. Polymerization of A_3-type monomers was conducted via acyclic triene metathesis polymerization and terminated before gelation. From NMR and SEC experiments the highly branched structure of the polymers was proven. These materials were then investigated with respect to their capability of actively reacting with singlet oxygen that is generated in many photoprocesses. We chose triplet−triplet annihilation photon upconversion as a highly oxygen-sensitive process to evaluate the performance of the different unsaturated polyesters. A structural optimum was found for **hb2** in upconversion efficiency and lifetime. From theoretical calculations the use of the phosphate central core was rationalized besides the obvious benefits of a potentially biodegradable polymer as a sustainable material for many applications. Also, measurements of the relaxation times of the protons, carbons, and phosphorus centers by NMR spectroscopy revealed the efficiency of the phosphates to react with singlet oxygen and to allow a long-term protection of many photonic processes where singlet oxygen could be generated. The combination of multiple end groups and the low viscosity in a hyperbranched polymer together with the phosphate central units makes the scavenging of singlet oxygen possible, while linear UPPEs do not work efficiently for this process. We believe that this development will find many applications ranging from drug carriers (phototherapy) to novel photovoltaic devices due to the high-efficiency, straightforward, and low-cost synthesis which is specially designed to remove singlet oxygen from any photoprocess without reacting with triplet oxygen.

EXPERIMENTAL SECTION

Chemicals. Phosphoryl chloride (99%) was purchased from Sigma-Aldrich and used as received. 3-Buten-1-ol (96%), 5-hexen-1-ol (98%), and 10-undecen-1-ol (98%) were purchased from Sigma-Aldrich and used as received. Triethylamine was dried over calcium hydride before use and stored under argon over 4 Å molecular sieves. All solvents were dried before use. The Grubbs first-generation catalyst was purchased from Sigma-Aldrich and stored under N_2. 3,9(10)-Dibromoperylene was synthesized as described before.[35] Column chromatography was performed on silica gel (Geduran Si60, Merck). Linear UPPE was synthesized as reported earlier.[18]

Methods. SEC measurements were carried out in THF, with samples of 1 g L^{-1} concentration. Sample injection was performed by a 717 plus autosampler (Waters) at 30 °C in THF. The flow rate was 1 mL min^{-1}. Three SDV columns (PSS) with dimensions of 300 × 80 mm, a 10 μm particle size, and pore sizes of 106, 104, and 500 Å were employed. Detection was accomplished with a DRI Shodex RI-101 detector (ERC) and UV−vis S-3702 detector (Soma). Calibration was carried out using polystyrene standards provided by the Polymer Standards Service. SEC-MALLS measurements were carried out at 30 °C in THF. An SDV column (PSS) with dimensions of 300 × 80 mm and pore sizes of linear M was employed. Detection was accomplished with a SECcurity DVD1260 4 capillary online viscosimeter (PSS).

The NMR experiments were recorded with a 5 mm BBI ^{1}H/X z-gradient on a 700 MHz spectrometer with a Bruker Avance III system. For the ^{1}H NMR spectrum 64 transients were used with an 11 μs long 90° pulse and a 12600 Hz spectral width together with a recycling delay of 5 s. The ^{13}C NMR (176 MHz) and ^{31}P NMR (283 MHz) measurements were obtained with a ^{1}H powergate decoupling method using a 30° flip angle, which had a 14.5 μs long 90° pulse for carbon and a 27.5 μs long 90° pulse for phosphorus. Additionally, carbon spectra were kept with a J-modulated spin−echo for ^{13}C nuclei coupled to ^{1}H to determine the number of attached protons with decoupling during acquisition. The spectral widths were 41660 Hz (236 ppm) for ^{13}C and 56818 Hz (200 ppm) for ^{31}P, both nuclei with a relaxation delay of 2 s. Similar 1D (^{1}H, ^{13}C, and ^{31}P NMR) measurements (^{1}H NMR (500 MHz), ^{31}C NMR (125.77 MHz), and ^{31}P NMR (202 MHz)) were made on a Bruker Avance III 500 NMR spectrometer with a 5 mm broad-band fluorine observation (BBFO) probe equipped with a z-gradient. The spectra were obtained with $\pi/2$ pulse lengths of 11.9 μs (^{1}H), 13.2 μs (^{13}C), and 11 μs (^{31}P) and a sweep width of 10330 Hz (20.6 ppm) for ^{1}H, 29700 Hz (236 ppm) for ^{13}C, and 40000 Hz (200 ppm) for ^{31}P, all nuclei with a relaxation delay of 2 s.

The "inversion recovery experiments" were used to measure the relaxation times of the protons, carbons, and phosphorus. For the measurements, relaxation delays of 20 s for protons, 20 s for phosphorus, and 40 s for carbons were needed. The pseudo-2D pulse program runs with eight scans with eight different echo times. The carbon and phosphorus relaxation time measurements used a power-gated decoupling to suppress the indirect coupling of the protons with the heteronuclei.

Matrix-assisted laser desorption and ionization time-of-flight (MALDI-ToF) measurements were obtained with a Shimadzu Axima CFR MALDI-ToF mass spectrometer, equipped with a nitrogen laser delivering 3 ns laser pulses at 337 nm. Dithranol (1,8,9-trishydroxyanthracene) was used as the matrix. Samples were prepared by dissolving the polymer in $CHCl_3$ at a concentration of 10 g L^{-1}. A 10 mL aliquot of this solution was added to 10 mL of a 10 g L^{-1} matrix solution and 1 mL of a potassium trifluoroacetic acid (KTFA) solution (0.1 M in methanol as the cationization agent). A 1 mL aliquot of the resulting mixture was applied to a multistage target to evaporate $CHCl_3$ and create a thin matrix/analyte film. The samples were measured in positive ion mode and in the linear mode of the spectrometer. The glass transition temperature was measured by differential scanning calorimetry (DSC) on a Mettler Toledo DSC 823 calorimeter. Three scanning cycles of heating−cooling were performed (N_2, 30 mL min^{-1}) with a heating rate of 10 °C min^{-1}.

Representative Procedure for Monomer Synthesis. To a dried three-necked, 250 mL round-bottom flask fitted with a dropping funnel were added 0.1 mol of the appropriate alcohol and 0.1 mol of triethylamine under an argon atmosphere in 80 mL of dry CH_2Cl_2. Then 0.03 mol of phosphoryl chloride dissolved in 20 mL of dry CH_2Cl_2 was added dropwise to the above flask at 0 °C. Then the reaction was allowed to warm to room temperature and stirred for an additional 12 h. The mixture was concentrated under reduced pressure, dissolved in diethyl ether, and filtered. The crude was washed twice with brine, and the organic layer was dried over anhydrous sodium sulfate, filtered, and concentrated in vacuo. The compounds were purified by chromatography over neutral alumina (or silica) using dichloromethane as the eluent or by distillation under reduced pressure to give clear, colorless oils. The purity and chemical structure were determined by ^{1}H NMR, ^{13}C NMR, and ^{31}P NMR spectroscopies as well as electrospray ionization mass spectrometry (ESI-MS).

Synthesis of Tribut-3-en-1-yl Phosphate (1). Following the general procedure described above and using 3-buten-1-ol, tribut-3-en-1-yl phosphate was obtained as a clear oil with a yield of 70% after column chromatography over neutral alumina using as the eluent dichloromethane (R_f = 0.7). ^{1}H NMR (500 MHz, $CDCl_3$): δ/ppm

dx.doi.org/10.1021/ja5049412 | J. Am. Chem. Soc. 2014, 136, 11057−11064

5.83−5.75 (m, 3H), 5.15−5.08 (m, 6H), 4.09−4.05 (m, 6H), 2.45−2.41 (m, 6H). ^{13}C NMR (126 MHz, $CDCl_3$): δ/ppm 133.50, 117.84, 66.89, 66.84, 34.80, 34.74. ^{31}P NMR (202 MHz, $CDCl_3$): δ/ppm −1.11. ESI-MS (m/z): 283.11 $[M + Na]^+$ (calcd for $C_{12}H_{21}O_4P$, 260.12).

Synthesis of Trihex-5-en-1-yl Phosphate (2). Following the general procedure described above and using 5-hexen-1-ol, trihex-5-en-1-yl phosphate was obtained as a clear oil with a yield of 80% after column chromatography over neutral alumina using dichloromethane as the eluent to give a colorless oil (R_f = 0.6). ^{1}H NMR (700 MHz, $CDCl_3$): δ/ppm 5.77 (m, 3H), 5.00−4.98 (m, 3H), 4.96−4.94 (m, 3H), 4.02 (q, J = 7 Hz, 6H), 2.07 (q, J = 7 Hz, 6H),1.68 (m, 6H), 1.47 (m, 6H). ^{13}C NMR (176 MHz, $CDCl_3$): δ/ppm 138.35, 115.01, 67.61, 67.57, 33.27, 29.84, 29.80, 24.84. ^{31}P NMR (283 MHz, $CDCl_3$): δ/ppm −0.67. ESI-MS (m/z): 345.23 $[M + H]^+$, 367.22 $[M + Na]^+$, 689.44 $[2M + H]^+$, 711.42 $[2M + Na]^+$ (calcd for $C_{18}H_{43}O_4P$, 344.21).

Synthesis of Triundec-10-en-1-yl Phosphate (3). Following the general procedure described above and using 10-undecen-1-ol, triundec-10-en-1-yl phosphate was obtained as a clear oil with a yield of 60% after column chromatography over neutral alumina using dichloromethane as the eluent to give a colorless oil (R_f = 0.5). ^{1}H NMR (700 MHz, $CDCl_3$): δ/ppm 5.77 (m, 3H), 5.00−4.98 (m, 3H), 4.93−4.91 (m, 3H), 4.02 (q, J = 7 Hz, 6H), 2.02 (q, J = 7 Hz, 6H), 1.66 (m, 6H), 1.36−1.27 (br, 36H). ^{13}C NMR (176 MHz, $CDCl_3$): δ/ppm 139.27, 114.26, 67.80, 67.76, 33.92, 30.45, 30.42, 29.59, 29.53, 29.27, 29.23, 29.05, 25.59. ^{31}P NMR (283 MHz, $CDCl_3$): δ/ppm −0.62. ESI-MS (m/z): 545.45 $[M + H]^+$, 577.44 $[M + Na]^+$ (calcd for $C_{33}H_{63}O_4P$, 544.45).

Representative Procedure for the ADMET Bulk Polymerization of 1, 2, and 3. In a dry Schlenk tube fitted with a magnetic stir bar was placed the monomer (2 mL) under an argon atmosphere. The temperature was raised to 60 °C, and the Grubbs first-generation catalyst (0.5 mol %) was added. After ethylene started to evolve, a controlled vacuum of 5 × 10^{-2} mbar was applied to remove the condensate. After 0.5 h, the reaction was cooled to room temperature, diluted with a solution containing tris(hydroxymethyl)phosphine (5 mol %) and triethylamine (5 mol %) in 10 mL of dry CH_2Cl_2, and stirred for 1 h. Then water was added, and stirring was continued for an additional 1 h to decolorize the brown solution. The mixture was extracted with CH_2Cl_2 and washed twice with brine. The organic layer was dried over anhydrous sodium sulfate, filtered, and concentrated in vacuo. The polymer, obtained with a quantitative yield, was then dissolved in the minimum volume of chloroform, precipitated into hexane or methanol (which is a nonsolvent for the polymer, but a good solvent for both monomers) when requested, and dried.

Synthesis of Polymer hb1. Tribut-3-en-1-yl phosphate (**1**) was reacted following the general procedure described above for ADMET bulk polymerization. ^{1}H NMR (700 MHz, $CDCl_3$): δ/ppm 5.81−5.76 (m, 3H), 5.52−5.53 (br, 3H), 5.15−5.09 (m, 6H), 4.08−4.00 (m, 13H), 2.46−2.39 (m, 13H). ^{13}C NMR (176 MHz, $CDCl_3$): δ/ppm 133.48, 128.31, 128.24, 128.20, 127.34, 127.28, 127.23, 117.88, 67.10, 66.89, 34.79, 34.75, 33.76, 28.75, 28.72. ^{31}P NMR (283 MHz, $CDCl_3$): δ/ppm −0.71, −1.05, −1.08, −1.11.

Synthesis of Polymer hb2. Trihex-5-en-1-yl phosphate (**2**) was reacted following the general procedure described above for ADMET bulk polymerization. ^{1}H NMR (700 MHz, $CDCl_3$): δ/ppm 5.81−5.75 (m, 3H), 5.38−5.35 (m, 6H), 5.02−4.95 (m, 6H), 4.04−4.00 (m, 16H), 2.09−2.00 (br, 16H),1.70−1.64 (br, 16H), 1.50−1.43 (br, 16H). ^{13}C NMR (176 MHz, $CDCl_3$): δ/ppm 138.36, 130.34, 129.80, 115.14, 115.03, 67.66, 67.62, 67.58, 33.28, 32.13, 30.07, 30.03, 29.93, 29.89, 29.84, 29.81, 26.84, 25.67, 25.51, 24.85. ^{31}P NMR (283 MHz, $CDCl_3$): δ/ppm −0.66 (br).

Synthesis of Polymer hb3. Triundec-10-en-1-yl phosphate (**3**) was reacted following the general procedure described above for ADMET bulk polymerization. ^{1}H NMR (700 MHz, $CDCl_3$): δ/ppm 5.83−5.73 (m, 3H), 5.37−5.34 (br, 7H), 5.00−4.92 (m, 6H), 4.04−4.00 (br, 19H), 2.04−1.95(br, 19H),1.66 (br, 19H), 1.36−1.28 (br, 125H). ^{13}C NMR (176 MHz, $CDCl_3$): δ/ppm 139.29, 130.45, 129.99, 114.29, 67.82, 67.80, 33.95, 32.78, 30.47, 29.84, 29.67, 29.62, 29.55, 29.35, 29.30, 29.07, 27.39. ^{31}P NMR (283 MHz, $CDCl_3$): δ/ppm 0.40, −0.62, −0.71.

Synthesis of 3,9(10)-Bis(3,3-dimethylbut-1-yn-1-yl)perylene (Y805). 3,9(10)-Dibromoperylene (410 mg, 1 mmol), $Pd(PPh_3)_4$ (100 mg), and CuI (30 mg) were added to a mixture of dry THF (15 mL) and dry piperidine (15 mL) in a 100 mL Schlenk flask. The flask was evacuated and flushed with argon several times. A 2-fold molar excess of 3,3-dimethylbutyne (330 mg, 4 mmol) was injected with a syringe. The mixture was heated to 80 °C and stirred for 14 h; the reaction mixture was poured into a 3-fold volume of ice/HCl (3:1). After the mixture was allowed to stand for 1 h, the yellow precipitate was filtered, rinsed with water, dried under vacuum, and purified by column chromatography on silica gel using toluene/heptane (1:2) as the eluent. Yield: 379 mg (92%). ^{1}H NMR (250 MHz, $C_2D_2Cl_4$, 25 °C, Me_4Si): δ/ppm 8.25 (t, J = 7.8 Hz, 2H), 8.18 (d, J = 8.3 Hz, 2H), 8.12 (t, J = 8.0 Hz, 2H), 7.66−7.57 (m, 4H), 1.45 (s, 18H). ^{13}C NMR (75 MHz, $C_2D_2Cl_4$): δ/ppm 134.41, 131.03, 130.82, 130.64, 130.58, 130.29, 128.00, 127.11, 127.07, 126.39, 126.28, 121.39, 121.30, 121.01, 120.86, 120.01, 119.87, 105.62, 77.19, 74.15, 74.04, 73.78, 73.41, 31.04. λ_{max}(toluene)/nm 479 (ϕ/ dm^3 mol^{-1} cm-1 51300), 447 (35500); fluorescence (toluene): λmax =486 nm (ϕ =54%, λ_{exc} = 480 nm). MS (FD, 8 kV) (m/z (rel intens)): 412.1 (100), M^+.

Represenative Procedure for the Upconversion Experiments Conducted in Hyperbranched UPPEs. The polymer films were prepared by mixing a stock solution of the dyes (in tetrahydrofuran) with the hyperbranched polymers. The obtained mixture was casted onto a glass surface and dried in vacuo at 40 °C for 48 h. The polymer films were prepared by the doctor blading technique on top of a cuvette (Hellma, type 106-QS). A cuvette of this type has deepening that allows a film with a thickness of 100 μm to be obtained. The dye concentration in the polymer films was determined by UV−vis spectroscopy, assuming that the extinction coefficient of the dyes in polymer films is similar to the extinction coefficient in toluene solution (the concentrations were C_{PdTBP} = 10^{-4} mol L^{-1} and $C_{emitter}$ = 2 × 10^{-3} mol L^{-1}). The details of the experimental setup for the measurements of TTA-UC spectra were reported earlier.[1]

Computational Details. Density functional theory (DFT) calculations were performed with the B3LYP[36,37] hybrid functional using the Gaussian09 package.[38] B3LYP is a hybrid generalized gradient exchange and correlation functional including exact exchange, and it has been extensively applied for studying the structure and reactivity of polymers. The geometries are fully optimized using a 6-311++G(3df,p) Gaussian basis set. A convergence criterion of 10^{-4} au on the gradient and displacement was imposed to determine equilibrium configurations. The residual root-mean-square (rms) force on all atoms was set to 10^{-5} hartree/bohr. The reaction path was investigated by performing a relaxed potential energy surface scan. The 6-311G(d,p) basis set was used to calculate the reaction barriers.

■ ASSOCIATED CONTENT

Ⓢ Supporting Information

Additional NMR spectra, thermal characterization, and additional photophysical characterization data. This material is available free of charge via the Internet at http://pubs.acs.org.

■ AUTHOR INFORMATION

Corresponding Author

wurm@mpip-mainz.mpg.de

Notes

The authors declare no competing financial interest.

■ ACKNOWLEDGMENTS

F.M. is a recipient of a fellowship through funding of the Excellence Initiative (Grant DFG/GSC 266) in the context of the Graduate School of Excellence "MAINZ" ("Materials Science in Mainz"). F.R.W. acknowledges the Deutsche

Forschungsgemeinschaft (Grant DFG-WU750/5-1) for support. R.P and D.D. acknowledge funding from the MPRG program of the Max Planck Society. S.B. acknowledges Reintegration Grant RG-09-0002(DRG-02/2) from the Bulgarian Science Fund for financial support.

REFERENCES

(1) DeRosa, M. C.; Crutchley, R. *J. Coord. Chem. Rev.* **2002**, *233*−*234*, 351.
(2) Zhao, J.; Wu, W.; Sun, J.; Guo, S. *Chem. Soc. Rev.* **2013**, *42*, 5323.
(3) Weston, M. A.; Patterson, M. S. *Photochem. Photobiol. Sci.* **2014**, *13*, 112.
(4) Weishaupt, K. R.; Gomer, C. J.; Dougherty, T. J. *Cancer Res.* **1976**, *36*, 2326.
(5) Islangulov, R. R.; Lott, J.; Weder, C.; Castellano, F. N. *J. Am. Chem. Soc.* **2007**, *129*, 12652.
(6) Tanaka, K.; Okada, H.; Ohashi, W.; Jeon, J.-H.; Inafuku, K.; Chujo, Y. *Biorg. Med. Chem.* **2013**, *21*, 2678.
(7) Chen, H.-C.; Hung, C.-Y.; Wang, K.-H.; Chen, H.-L.; Fann, W. S.; Chien, F.-C.; Chen, P.; Chow, T. J.; Hsu, C.-P.; Sun, S.-S. *Chem. Commun.* **2009**, 4064.
(8) Wohnhaas, C.; Turshatov, A.; Mailänder, V.; Lorenz, S.; Baluschev, S.; Miteva, T.; Landfester, K. *Macromol. Biosci.* **2011**, *11*, 772.
(9) Liu, Y.; Chen, M.; Cao, T.; Sun, Y.; Li, C.; Liu, Q.; Yang, T.; Yao, L.; Feng, W.; Li, F. *J. Am. Chem. Soc.* **2013**, *135*, 9869.
(10) Liu, Q.; Yang, T.; Feng, W.; Li, F. *J. Am. Chem. Soc.* **2012**, *134*, 5390.
(11) Miteva T.; Fuhrmann G.; Nelles G.; Yakutkin V.; Balouchev, S. Organic Polymeric Photon Up-Conversion Nanoparticles for Biological Applications. US 8,431,051 B2, April 30, 2013.
(12) Baluschev, S.; Miteva, T.; Yakutkin, V.; Nelles, G.; Yasuda, A.; Wegner, G. *Phys. Rev. Lett.* **2006**, *97*, 143903.
(13) Keivanidis, P. E.; Baluschev, S.; Miteva, T.; Nelles, G.; Scherf, U.; Yasuda, A.; Wegner, G. *Adv. Mater.* **2003**, *15*, 2095.
(14) Borjesson, K.; Dzebo, D.; Albinsson, B.; Moth-Poulsen, K. *J. Mater. Chem. A* **2013**, *1*, 8521.
(15) Cheng, Y. Y.; Khoury, T.; Clady, R. G. C. R.; Tayebjee, M. J. Y.; Ekins-Daukes, N. J.; Crossley, M. J.; Schmidt, T. W. *Phys. Chem. Chem. Phys.* **2010**, *12*, 66.
(16) Steinbach, T.; Alexandrino, E. M.; Wurm, F. R. *Polym. Chem.* **2013**, *4*, 3800.
(17) Marsico, F.; Turshatov, A.; Weber, K.; Wurm, F. R. *Org. Lett.* **2013**, *15*, 3844.
(18) Marsico, F.; Wagner, M.; Landfester, K.; Wurm, F. R. *Macromolecules* **2012**, *45*, 8511.
(19) Wurm, F.; Frey, H., Hyperbranched Polymers: Synthetic Methodology, Properties, and Complex Polymer Architectures. In *Polymer Science: A Comprehensive Reference*; Matyjaszewski, K., Möller, M., Eds.; Elsevier: Amsterdam, 2012; Vol. *6*, pp 177−198.
(20) Wurm, F.; Frey, H. *Prog. Polym. Sci.* **2011**, *36*, 1.
(21) Darley, E. S. R.; MacGowan, A. P. *J. Antimicrob. Chemother.* **2004**, *53*, 928.
(22) Gao, C.; Yan, D. *Prog. Polym. Sci.* **2004**, *29*, 183.
(23) Gorodetskaya, I. A.; Choi, T.-L.; Grubbs, R. H. *J. Am. Chem. Soc.* **2007**, *129*, 12672.
(24) Ding, L.; Qiu, J.; Lu, R.; Zheng, X.; An, J. *J. Polym. Sci., Polym. Chem.* **2013**, *51*, 4331.
(25) del Río, E.; Lligadas, G.; Ronda, J. C.; Galià, M.; Cádiz, V.; Meier, M. A. R. *Macromol. Chem. Phys.* **2011**, *212*, 1392.
(26) Biermann, U.; Metzger, J. O.; Meier, M. A. R. *Macromol. Chem. Phys.* **2010**, *211*, 854.
(27) Mutlu, H.; de Espinosa, L. M.; Meier, M. A. R. *Chem. Soc. Rev.* **2011**, *40*, 1404.
(28) Wurm, F.; Lopez-Villanueva, F.-J.; Frey, H. *Macromol. Chem. Phys.* **2008**, *209*, 675.
(29) Filatov, M.; Baluschev, S.; Ilieva, I.; Enkelmann, V.; Miteva, T.; Landfester, K.; Cheprakov, A. *J. Org. Chem.* **2012**, *77*, 11119.
(30) Turshatov, A.; Busko, D.; Avlasevich, Y.; Miteva, T.; Landfester, K.; Baluschev, S. *ChemPhysChem* **2012**, *13*, 3112.
(31) Jason, D. P.; Brian, G. O.; Justin, P. B.; Mohammad, K. H.; Jo Ann, R.; Jeffrey, S. W.; James, W. R.; Sergei, N. High-Oxygen Barrier Materials Based on Hyperbranched Aliphatic Polyesters. *Polymer Degradation and Performance*; American Chemical Society: Washington, DC, 2009; Vol. *1004*, pp 17−30.
(32) Di Mascio, P.; Kaiser, S.; Sies, H. *Arch. Biochem. Biophys.* **1989**, *274*, 532.
(33) Foote, C. S. *Acc. Chem. Res.* **1968**, *1*, 104.
(34) Kearns, D. R. *Chem. Rev.* **1971**, *71*, 395.
(35) Schlichting, P.; Rohr, U.; Müllen, K. *Liebigs Ann.* **1997**, *1997*, 395.
(36) Becke, D. A. *Phys. Rev. A* **1988**, *38*, 3098.
(37) Lee, C.; Yang, W.; Parr, R. G. *Phys. Rev. B* **1988**, *37*, 785.
(38) Frisch, M. J.; Trucks, G. W.; Schlegel, H. B.; Scuseria, G. E.; Robb, M. A.; Cheeseman, J. R.; Scalmani, G.; Barone, V.; Mennucci, B.; Petersson, G. A.; Nakatsuji, H.; Caricato, M.; Li, X.; Hratchian, H. P.; Izmaylov, A. F.; Bloino, J.; Zheng, G.; Sonnenberg, J. L.; Hada, M.; Ehara, M.; Toyota, K.; Fukuda, R.; Hasegawa, J.; Ishida, M.; Nakajima, T.; Honda, Y.; Kitao, O.; Nakai, H.; Vreven, T.; Montgomery, J. A., Jr.; Peralta, J. E.; Ogliaro, F.; Bearpark, M.; Heyd, J. J.; Brothers, E.; Kudin, K. N.; Staroverov, V. N.; Kobayashi, R.; Normand, J.; Raghavachari, K.; Rendell, A.; Burant, J. C.; Iyengar, S. S.; Tomasi, J.; Cossi, M.; Rega, N.; Millam, J. M.; Klene, M.; Knox, J. E.; Cross, J. B.; Bakken, V.; Adamo, C.; Jaramillo, J.; Gomperts, R.; Stratmann, R. E.; Yazyev, O.; Austin, A. J.; Cammi, R.; Pomelli, C.; Ochterski, J. W.; Martin, R. L.; Morokuma, K.; Zakrzewski, V. G.; Voth, G. A.; Salvador, P.; Dannenberg, J. J.; Dapprich, S.; Daniels, A. D.; Farkas, Ö.; Foresman, J. B.; Ortiz, J. V.; Cioslowski, J.; Fox, D. J. *Gaussian09*; Gaussian, Inc.: Wallingford, CT, 2009.